Nuclear Science and Techniques (2025) 36:105
https://doi.org/10.1007/s41365-025-01683-7

Many-objective evolutionary algorithms based on reference-point-selection strategy for application in reactor radiation-shielding design

Cheng-Wei Liu[1,2] · Ai-Kou Sun[1,2] · Ji-Chong Lei[1,2] · Hong-Yu Qu[1,2] · Chao Yang[1,2] · Tao Yu[1,2] · Zhen-Ping Chen[1,2]

Received: 12 February 2024 / Revised: 3 June 2024 / Accepted: 10 June 2024 / Published online: 22 April 2025

Abstract

In recent years, the development of new types of nuclear reactors, such as transportable, marine, and space reactors, has presented new challenges for the optimization of reactor radiation-shielding design. Shielding structures typically need to be lightweight, miniaturized, and radiation-protected, which is a multi-parameter and multi-objective optimization problem. The conventional multi-objective (two or three objectives) optimization method for radiation-shielding design exhibits limitations for a number of optimization objectives and variable parameters, as well as a deficiency in achieving a global optimal solution, thereby failing to meet the requirements of shielding optimization for newly developed reactors. In this study, genetic and artificial bee-colony algorithms are combined with a reference-point-selection strategy and applied to the many-objective (having four or more objectives) optimal design of reactor radiation shielding. To validate the reliability of the methods, an optimization simulation is conducted on three-dimensional shielding structures and another complicated shielding-optimization problem. The numerical results demonstrate that the proposed algorithms outperform conventional shielding-design methods in terms of optimization performance, and they exhibit their reliability in practical engineering problems. The many-objective optimization algorithms developed in this study are proven to efficiently and consistently search for Pareto-front shielding schemes. Therefore, the algorithms proposed in this study offer novel insights into improving the shielding-design performance and shielding quality of new reactor types.

Keywords Many-objective optimization problem · Evolutionary algorithm · Radiation-shielding design · Reference-point-selection strategy

1 Introduction

Radiation-shielding designs for reactors aim to minimize the external radiation dose (ALARA) by selecting appropriate shielding materials and structures to meet the radiation-safety requirements of the personnel [1, 2]. Additionally, with the development of new types of nuclear reactors in various fields, the shielding design needs to balance safety standards with the consideration of miniaturization and lightweight design, such as for marine, transportable, and space reactors [2–5]. Consequently, the radiation-shielding design for newly developed reactors presents a typical multi-objective optimization problem, as it involves multiple design objectives and parameters, including the radiation dose, volume, and weight (Fig. 1).

This work was supported by the National Natural Science Foundation of China (Nos. 12475174 and 12175101) and YueLuShan Center Industrial Innovation (No. 2024YCII0108).

✉ Zhen-Ping Chen
chzping@usc.edu.cn

[1] School of Nuclear Science and Technology, University of South China, Hengyang 421001, China

[2] Key Lab of Advanced Nuclear Energy Design and Safety, Ministry of Education, University of South China, Hengyang 421000, China

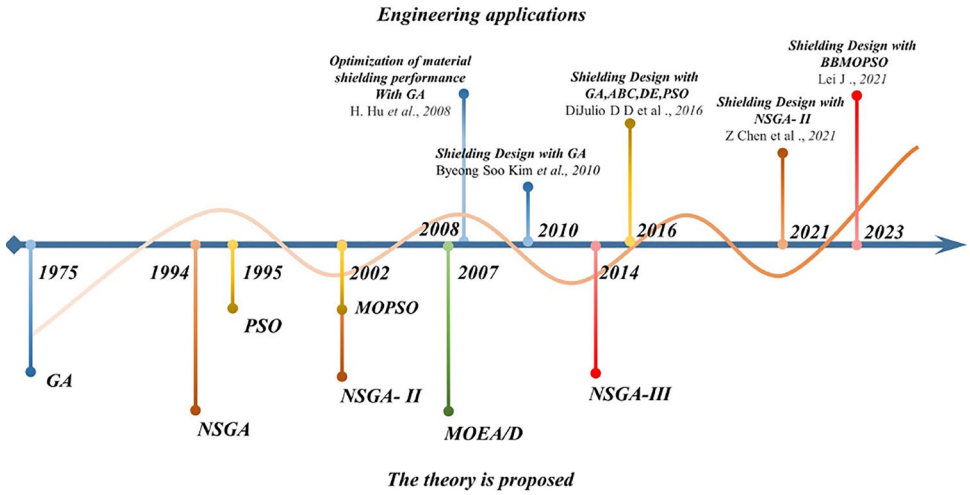

Fig. 1 (Color online) Application of evolutionary algorithms in reactor-shielding design

Conventional shielding-design methods rely heavily on expert knowledge, and require manual iterations to achieve acceptable results. With the development of evolutionary optimization algorithms, some researchers have begun to employ single-objective optimization algorithms, such as the genetic algorithm (GA), particle swarm optimization, and differential evolution, to optimize the radiation dose as a single objective [5–7]. In recent years, studies have also utilized multi-objective (two or three objectives) optimization algorithms, such as the non-dominated sorting genetic algorithm II (NSGA-II) and multi-objective particle swarm optimization, to optimize the volume-dose trade-off as multiple objectives [8–12]. This means that evolutionary algorithms have received considerable attention and can provide new opportunities for complex shielding-optimization problems.

However, in practical shielding-optimization designs, the number of objectives to be optimized often exceeds four, resulting in a typical many-objective problem (four or more objectives to be optimized) [13, 14]. Conventional multi-objective optimization algorithms exhibit suboptimal performance when dealing with many-objective optimization problems [15, 16], failing to meet the requirements of achieving a global optimal solution in the shielding design. Therefore, in this study, we propose a reference point-based many-objective artificial bee-colony algorithm (RP-MOABC) and reference point-based non-dominated sorting algorithm (RP-NSGA) to solve many-objective shielding-optimization problems.

The remainder of this paper is organized as follows. Section 2 presents the mathematical model of the many-objective optimization problem in reactor radiation shielding and discusses the encoding methods for shielding design. In Sect. 3, we provide an overview of the fundamental principles of the proposed genetic-and bee-colony-based optimization algorithms. We also outline a detailed framework for their application in radiation-shielding designs. Section 4 presents the numerical models of reactor-shielding design applications, along with the corresponding numerical results. Finally, the concluding section summarizes the key findings and conclusions of this study.

2 Many-objective optimization problem in reactor radiation-shielding design

This section provides a concise overview of reactor radiation-shielding design and the associated mathematical model for the many-objective shielding-optimization problem. It begins with a brief explanation of the principles underlying the shielding design for neutrons and gamma rays in reactors. Next, a mathematical model is proposed to address the many-parameter, many-objective, and many-constraint reactor-shielding design. Finally, a special encoding method is proposed to represent the shielding parameters (such as the number of shielding layers, types of shielding materials, and their compositions), facilitating the optimization process.

2.1 Principles of radiation-shielding design

The primary objective of reactor radiation shielding is to design a shielding system composed of multilayer and multi-material structures that surround the core facilities within the reactor, ensuring that the personnel are in an environment where the radiation dose meets the specified limits. This is achieved by utilizing suitable shielding materials and geometric configurations combined with multilayered and multi-component structures to shield the radiation sources. The selection and arrangement of materials in each layer are based on their specific shielding capabilities and nuclear interactions with radiation particles, with the aim of minimizing radiation levels to the maximum possible extent.

The principles governing the design of radiation shielding are based on the interactions between the radiation particles

and materials. Radiation predominantly comprises neutrons and gamma rays. Neutron interactions include absorption and scattering, which is further categorized into elastic and inelastic scattering. For neutron shielding, the secondary gamma rays generated during inelastic scattering reactions must be considered. The interactions of gamma rays include Compton scattering, photoelectric absorption, and pair production. Typically, neutron shielding requires materials containing heavy and light isotopes, such as light water, boron carbide, and polyethylene [17, 18]. Conversely, gamma-ray shielding requires materials with high-Z isotopes, including lead, concrete, and steel [19].

2.2 Many-objective mathematical model for radiation-shielding design

Many-objective optimization in practical applications aims to achieve multiple optimized objectives within specific constraints. However, owing to the inherent conflicts between these objectives, optimizing one objective is typically achieved at the expense of deteriorating the others. As a result, a unique optimal solution is elusive; instead, a set of Pareto-front solutions consisting of non-dominated individuals is obtained [20]. Radiation-shielding design presents a typical many-objective optimization problem in nuclear engineering. The goal is to minimize the mass and volume of the total shielding system while ensuring that the external radiation dose satisfies the ALARA principle. However, weight, volume, and radiation dose are conflicting objectives that cannot be optimized simultaneously. In this study, we focus on minimizing the total weight, total volume, and axial and radial radiation doses outside the shielding layers. These objectives are influenced by various parameters, including the thickness of the shielding layer, materials used, and the composition of the materials used. Additionally, constraints are imposed on the fast-neutron, thermal-neutron, and gamma-ray flux rates outside the shielding layers during the optimization process. Reactor radiation-shielding design involves many objectives, parameters, and constraints. To address these challenges, the mathematical model in Eq. (1) is proposed:

$$\begin{cases} \min F(X) = (F_{\mathrm{R}}(X), F_{\mathrm{W}}(X), F_{\mathrm{V}}(X))^{\mathrm{T}} \\ s.t. \begin{cases} F_{\mathrm{R}}(X) = R_{\mathrm{N}}(X) + R_{\mathrm{P}}(X) \le R_0 \\ F_{\mathrm{W}}(X) = \sum_{m=1}^{M} V_m \cdot \rho_m \le W_0 \\ F_{\mathrm{V}}(X) = \sum_{m=1}^{M} V_m \le V_0 \\ \Phi_{\mathrm{N}}(X) \le \Phi_{\mathrm{N}_0} \\ \Phi_{\mathrm{P}}(X) \le \Phi_{\mathrm{P}_0} \\ X = (x_1, x_2, x_3, \ldots, x_{n-1}, x_n), X \in \mathfrak{R} \\ L_i \le x_i \le U_i (i = 1, 2, \ldots, n) \\ . \end{cases} \end{cases} \tag{1}$$

Based on the optimization model (1), where X is the decision variable in the shielding design (geometry thickness, material type, material composition), the values L_i and U_i represent the lower and upper bounds of the variables, respectively; the vector space containing all decision variables is represented by X; and $\Phi_{\mathrm{N}}(X)$ and $\Phi_{\mathrm{P}}(X)$ represent the neutron and photon flux rates outside the shielding layer, respectively, while Φ_{N_0} and Φ_{P_0} are their corresponding constraint values; V_m represents the volume of the m-th shielding layer, and ρ_m represents the corresponding density of the shielding material denoted by m. W_m is the mass of the shielding layers; R_{N} and R_{P} represent the neutron and photon dose external to the shielding layer, respectively; $F_{\mathrm{R}}(X)$, $F_{\mathrm{W}}(X)$, and $F_{\mathrm{V}}(X)$ represent the radiation dose of the shielding layer and the total weight and total volume of the shielding system, respectively; R_0, W_0, and V_0 represent the constraints for the radiation dose, weight, and volume, respectively; $F(X)$ is the radiation-shielding design objective vector, and the minimized value is expected to be optimized for each dimension of the objective vector.

2.3 Encoding methods of radiation-shielding model

In recent years, the development of radiation-shielding designs has progressed significantly, and a series of studies combining evolutionary algorithms with various types of shielding designs have emerged. However, the decision vector in this type of research only covers the shielding structure and shielding-material-type changes, and no material-composition-optimization research has been previously carried out. In this study, the reactor-shielding model is simulated for the many-parameter problem in shielding optimization using both binary encoding and real-number encoding, which can be encoded to characterize the shielding-model geometry, material type, and material composition, and coupled with a variety of evolutionary algorithms for calculation.

Figure 2 illustrates the encoding process for the simple shielding scheme. First, the thicknesses of the shielding layers and the corresponding index numbers for the shielding materials are obtained. The composition is determined for materials with variable compositions, such as borated and lead-borated polyethylene. Second, the above parameters are encoded in real or binary numbers. The composition content, which is subject to fixed-sum constraints, is transformed using spherical-coordinate conversion [21], as in Eq. (2) prior to encoding. Finally, the encoding design is completed for all shielding layers. The purpose of encoding is to combine the shielding model with the evolutionary algorithm such that the model parameters can be optimized by the algorithm, and the final shielding scheme can be obtained for the reference of the designer.

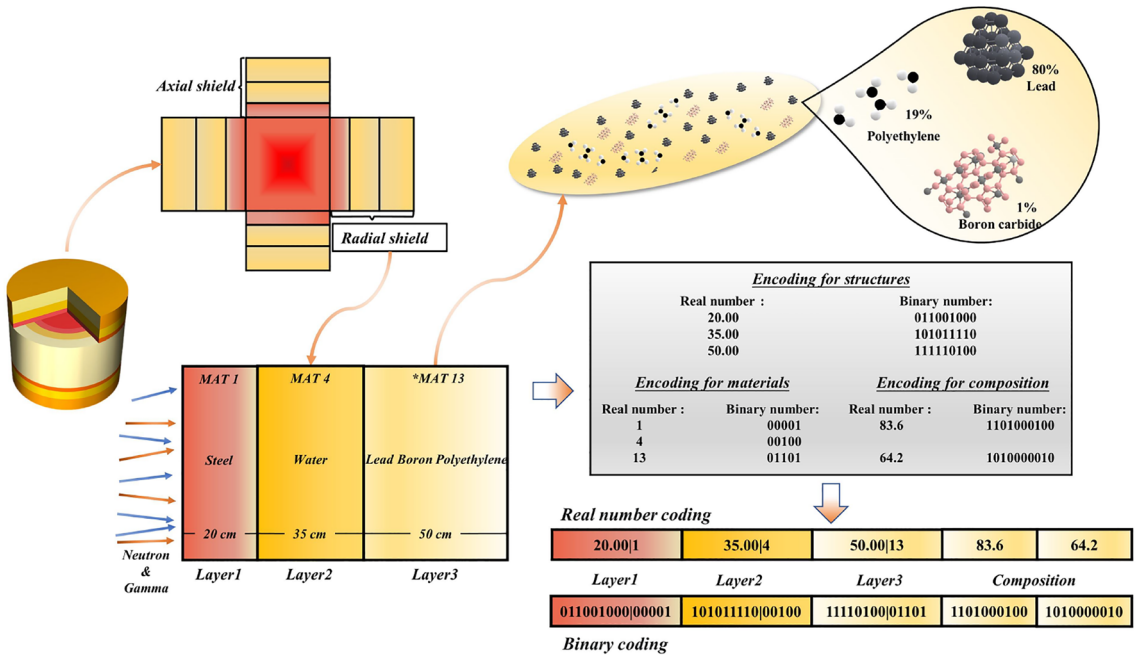

Fig. 2 (Color online) Example of the encoding method for a radiation-shielding model

$$
\begin{aligned}
x_i &= (\sin\theta_1 \cdot \sin\theta_2 \ldots \sin\theta_{n-1})^2, i = 1 \\
x_i &= (\cos\theta_{i-1} \cdot \sin\theta_i \ldots \sin\theta_{n-1})^2, i = 2, \ldots, n-1 \\
x_i &= (\cos\theta_{n-1})^2, i = n
\end{aligned} \tag{2}
$$

3 Many-objective evolutionary algorithms for radiation-shielding design

3.1 Scheme of radiation-shielding optimization with many-objective evolutionary algorithm

In this study, shielding-optimization methods are proposed by combining many-objective evolutionary algorithms with particle-transport calculation software that can optimize the reactor primary-shielding structures, material types, and material compositions to obtain optimal shielding-design schemes through an automated process. These methods are embedded into the multi-functional radiation-transport simulation platform (MOSRT) developed by the NEAL team [22, 23].

A schematic of the many-objective optimization of the radiation-shielding design is shown in Fig. 3, and the steps are described as follows.

(1) Preprocessing of the initial shielding model is performed using the MOSRT software. First, the CAD model of the reactor geometry is modeled with MOSRT, and the model is automatically converted into a particle-transport calculation model. The shielding regions to be optimized are labeled. Finally, the initial running parameters are set, including the maximum number of iterations g, population size N, and optimization-objective number M.

(2) The evolutionary algorithm is selected. In this study, the genetic and ABC algorithms are invoked as evolutionary algorithms to optimize the weight, volume, and region-specific radiation-dose rate of the reactor radiation-shielding model.

(3) The decision-vector encoding method (real-number encoding or binary encoding) is chosen based on the requirements, and the initial parent population $P_{g=1}$ is generated.

(4) The initial offspring population $Q_{g=1}$ is generated based on the parent-population characteristics. The GA uses selection, crossover, and mutation to generate the offspring population, and the bee-colony algorithm uses employed, onlooker, and scout bees to update the offspring population. The parent population P_g is merged with the offspring population Q_g to obtain the g-th generation combined population C_g. The population is decoded and converted into a particle-transport input card to solve the objective values. The MOSRT has a built-in shielding-calculation module integrated with the Monte Carlo method (MC) [24].

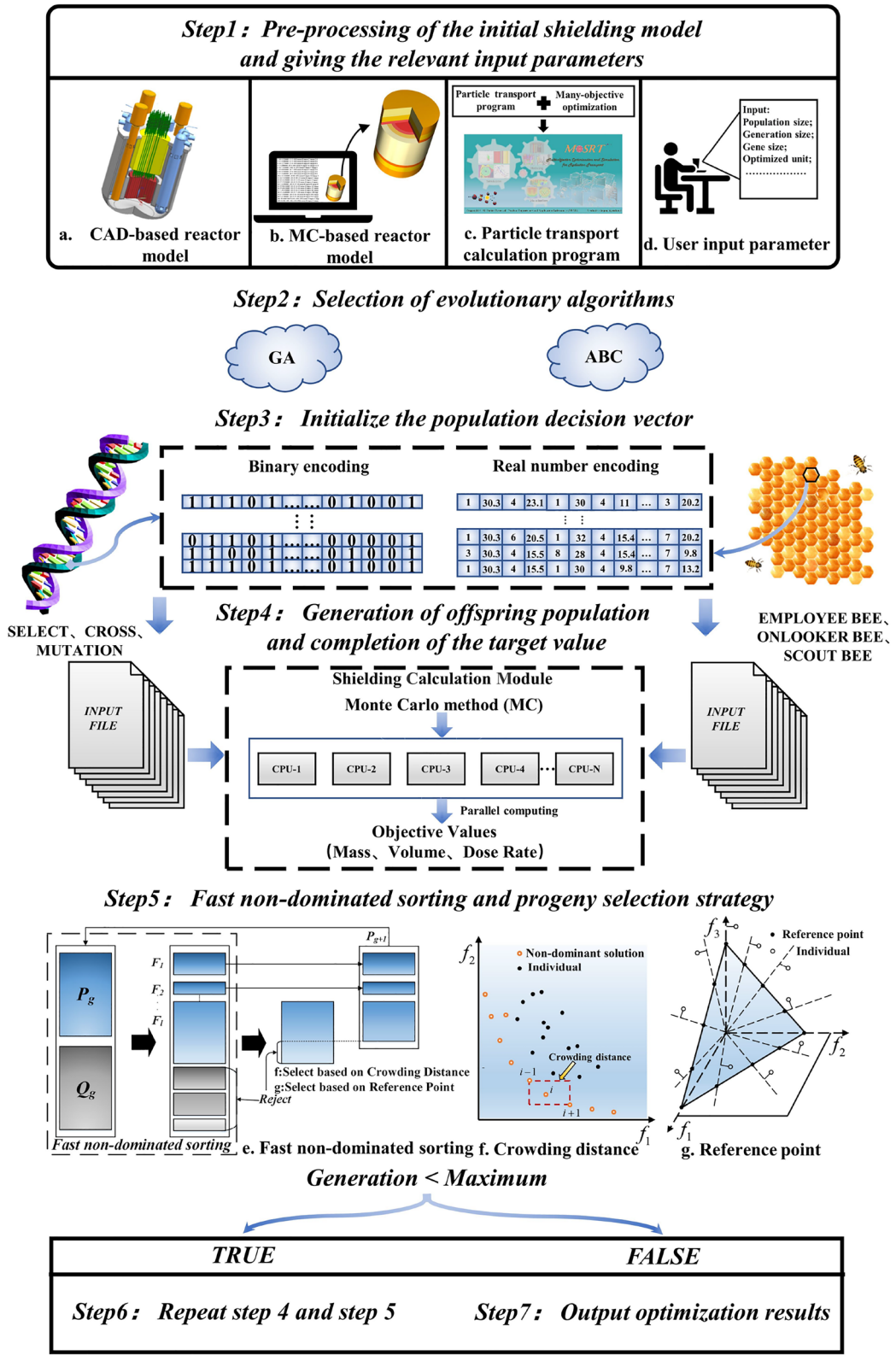

Fig. 3 (Color online) Schematic of radiation-shielding design with many-objective evolutionary algorithm

(5) A fast non-dominated sorting strategy is applied to the merged population, and each algorithm uses the reference-point-selection strategy [25] to generate the new parent population P_{g+1}. A performance-comparison analysis is conducted simultaneously with conventional methods that use crowding-distance strategy selection [26]. Specific strategies are explained in Sect. 3.5.
(6) Steps (4) and (5) are repeated if the maximum number of iterations is not reached, and the parent population P_{g+1} is continuously updated; otherwise, step (7) is implemented.
(7) The optimization process is completed, and the optimization results of each algorithm are thoroughly compared and analyzed.

3.2 Evolutionary strategy based on genetic algorithm

The GA [27] is a classical evolutionary strategy for simulating inheritance and evolution in nature. It searches for the solution space of optimization problems through operations such as selection, crossover, and mutation. GAs based on different evaluation strategies exhibit significant differences in performance when solving various problems [28]. The following section explains the basic operations of GAs.

Selection: In this study, a binary tournament-selection operation is used, where two individuals (the individual in the paper means a specific shielding scheme) are taken from the current population at a time, the dominance relationship between the two individuals is judged, and the individual in the dominant position is selected for subsequent crossover and mutation. If two individuals do not dominate each other, one individual is randomly selected for the subsequent genetic steps. The determination of the dominance relationship will be explained in Sect. 3.4.1.

Crossover: The crossover operation mimics the process of hybridization in biological evolution. It selects the chromosomal segments (genes) of two or more parent individuals for exchange to generate new offspring. In this study, we use a single-point crossover operation for GAs with binary encoding and a simulated binary crossover operation for GAs with real-number encoding.

Mutation: The mutation operation introduces a degree of randomness to the algorithm by changing some gene values on individual chromosomes to generate new individuals. The mutation operation can increase the diversity of the population and prevent it from falling into a locally optimum solution. The mutation operation can randomly select some genes of an individual to be changed or mutate each gene on the chromosome with a particular probability. In this study, we use the bit-flip mutation operation for GAs with binary encoding and polynomial mutation operations for GAs with real-number encoding.

3.3 Evolutionary strategy based on artificial bee-colony algorithm

The ABC [29, 30] algorithm is a global optimization technique based on swarm intelligence. It draws inspiration from the foraging behavior of bee colonies, where individual bees perform specific tasks and share information to collectively find the optimal solution to a problem. This study builds on the fundamental ABC algorithm and introduces improvements by employing two methods: a differential evolution search [31] and golden sine search [32]. The following sections explain the search strategies of the algorithm.

Employed bee search: In this phase, a number of hired bees consistent with the population size will be dispatched to search for historical food sources (solution space). In this study, the bee population searches using a differential-search method based on an elite strategy. Individuals in the Pareto optimal set (the Pareto optimal set will be explained in Sect. 3.4.2.) are randomly used as bootstrap terms, and the differential evolution operator is used to generate new solutions, as shown in Eq.(3):

$$X^t = X^{t1} + R\left(X^{t1} - X^{t2}\right) + R\left(X^{t1} - X^{t3}\right), \tag{3}$$

where X^{t1}, X^{t2}, and X^{t3} are three mutually dissimilar solutions selected from the Pareto optimal set and R are random numbers between [0, 1].

The elite-guided search mechanism is an exploitation operation that unavoidably reduces the diversity of the population and may cause the algorithm to converge locally. To better balance the global-search and local-exploitation capabilities, this study proposes a solution-space search method based on the golden sine function:

$$\begin{aligned} X^t &= X_i|\sin(r_1)| + r_2 \cdot \sin(r_1) \cdot |c_1 X^{t1} - c_2 X_i|, \\ c_1 &= a g_s + b(1 - g_s), \\ c_2 &= a(1 - g_s) + b g_s. \end{aligned} \tag{4}$$

In Eq. (4), X_i represents the i-th individual, r_1 and r_2 are random numbers belonging to $[0, 2\pi]$ and $[0, \pi]$, respectively, c_1 and c_2 are introduced as golden section coefficients in the position-update formula, respectively, and a and b are initial values set to $-\pi$ and π, respectively. The golden section number g_s is $(\sqrt{5} - 1)/2$.

The employed bees use Eq. (3) and Eq.(4) for searching with equal probabilities to balance the diversity and local-search capability of the population.

Onlooker bee search: The onlooker bees perform repeated optimization on the excellent food sources based on the roulette-wheel selection. The specific optimization operations are the same as those of the employed bees, and the onlooker-bee evaluation function is as follows:

$$fit_i = \frac{dom}{FoodNumber}, \tag{5}$$

where *dom* represents the number of solutions in which the *i*-th feasible solution dominates among all feasible solutions, and *FoodNumber* represents the total number of food sources.

The roulette-wheel selection probability is defined as

$$p_i = \frac{fit_i}{\sum_{n=1}^{FoodNumber} fit_n}. \tag{6}$$

Food sources with higher probabilities have a greater probability of being explored in the subsequent bee stage, thereby facilitating the algorithm's efficient exploration of the space for excellent solutions.

Scout bee search: A food source is randomly selected from the last Pareto layer, its decision vector is randomized, and its corresponding objective values are reset.

3.4 Evaluation method of shielding scheme based on Pareto domination

3.4.1 Pareto domination of the shielding schemes

When evaluating the performance of different shielding-design schemes, in the case of a single objective (such as shield weight), a smaller shield weight indicates better performance of the design scheme. However, for multiple objectives, each shielding-design scheme has multidimensional attributes (such as shield weight, volume, and dose rate). The performance of shielding schemes cannot be evaluated simply based on numerical magnitudes.

First, the decision vectors must be decoded and converted into particle-transport program-input files, and the population objective values are calculated using the particle-transport program, as shown in Eq. (7):

$$D_{\text{pop}} = \begin{bmatrix} X_1 = [x_{1,1}x_{1,2}.....x_{1,n}] \\ ... \\ ... \\ ... \\ X_N = [x_{N,1}x_{N,2}.....x_{N,n}] \end{bmatrix}$$
$$\Downarrow \tag{7}$$
$$F_{\text{pop}} = \begin{bmatrix} F(X_1) = [F_{1,1}F_{1,2}.....F_{1,M}] \\ ... \\ ... \\ ... \\ F(X_N) = [F_{N,1}F_{N,2}.....F_{N,M}] \end{bmatrix}.$$

In this study, the performance evaluation method for the shielding-design schemes is based on the Pareto-domination method. Specifically, when a Pareto-domination relationship exists between the two schemes, the scheme in the dominant position performs better than the other schemes in the dominant position. For any two schemes X_u and X_v in a set of schemes, X_u dominates X_v if Eq. (8) is satisfied:

$$Dom(X_u, X_v) = \text{if} \begin{cases} F(X_u) \neq F(X_v) \\ W(X_u) \leq W(X_v) \\ V(X_u) \leq V(X_v) \\ R(X_u) \leq R(X_v) \end{cases} \Rightarrow X_u \prec X_v. \tag{8}$$

For constrained optimization problems, we employ the feasibility rule [33] to assess the superiority of the schemes. First, the feasibility of the scheme with respect to the constraints is evaluated. If the constraints are satisfied, then the constraint variable $Res(X)$ is set to zero; otherwise, it is set to one. When comparing two schemes X_u and X_v with the same value of $Res(X)$, the domination judgment is based on Eq. (8). However, when the two schemes have unequal values of $Res(X)$, the scheme with a value of 0 dominates that with a value of 1, as shown in Eq. (9) and (10):

$$Res(X) = \begin{cases} 0 & \text{if } r(X) \leq r_0(X) \\ 1 & \text{else} \end{cases} \tag{9}$$

$$Dom_{\text{res}}(X_u, X_v) = \begin{cases} Dom(X_u, X_v) & \text{if } Res(X_u) = Res(X_v) \\ X_u \prec X_v & \text{else if } Res(X_u) < Res(X_v) \\ X_v \prec X_u & \text{else,} \end{cases} \tag{10}$$

where $r_0(X)$ is the constraint vector and $r(X)$ is the constraint value of the corresponding individual.

3.4.2 Fast non-dominated sorting strategy

Based on the Pareto-domination judgment method, fast non-dominated sorting (Fig. 3e) of the populations can be performed to divide the different levels of the non-dominated layers. First, all schemes in the population are judged for domination, and all schemes that are not dominated by others are removed from the population and constitute the non-dominated layer F_1. Then, the population that eliminates the schemes in F_1 is again judged for domination, and all non-dominated schemes are removed from the population to constitute F_2. This is repeated until all the schemes are deposited in the non-dominated layer of the corresponding rank.

The schemes at each level of the non-dominated layer are not dominated by each other, and the smaller the level of the non-dominated layer, the better the integrated performance

of the schemes in the layer. The F_1 non-dominated layer is called the Pareto optimal set.

3.5 Pareto-set-selection strategy

When offspring are generated, the parent set P_g and resulting offspring set Q_g are combined into a set C_g. The schemes at the smaller non-dominant level of the set are selected to enter the next generation until all schemes at level F_l are selected to P_{g+1}, such that P_{g+1} is equal in size to P_g. If all the individuals at level F_l are selected to P_{g+1}, the next-generation population P_{g+1} is larger than P_g. Therefore, a certain strategy is required to select individuals at level F_l. In this study, crowding distance and reference-point-selection strategies are used. The details are as follows.

3.5.1 Selection strategy based on crowding distance

Conventional multi-objective optimization algorithms use the crowding distance to compare schemes in non-dominated layers. Further judgment is made by calculating the *CD* value for each scheme. The calculation method is given in Eq. (11) and Fig. 3f:

$$CD_i = \begin{cases} \infty & i = (1 \quad \text{or} \quad n) \\ \sum_{j=1}^{M} \frac{F_{i+1,j} - F_{i-1,j}}{F_j^{\max} - F_j^{\min}} & i = (2, ..., n-1) \end{cases} \quad j = (1, ..., M). \tag{11}$$

By summing the normalized distance of each scheme in each dimension of the objective space, we can determine whether the scheme has diversity in the current non-dominated layer. A scheme with a larger value of *CD* represents fewer similar schemes and is more likely to be selected for the next generation.

3.5.2 Selection strategy based on reference point

In the reference-point-selection strategy [34, 35], the reference points are first predefined in the normalized hyperplane and the number of reference points should be close to the population size, which is defined by Eq. (12):

$$RefCount = \begin{pmatrix} H + M - 1 \\ H \end{pmatrix} = C_{H+M-1}^{H}, \tag{12}$$

where M denotes the number of optimization objectives and H denotes the number of divisions. A schematic of the reference points in the case of three objectives and six divisions is shown in Fig. 4. The purpose of generating reference points is to generate a set of reference vectors in the objective space, through which schemes in the population can be associated with ensure that the diversity of the population is maintained during subsequent evolution.

We define S_g as the set consisting of all schemes in the F_1–F_l layers and adaptively normalize all schemes in S_g to the hyperplane. First, we define the ideal point $z = (z_1^{\min}, z_2^{\min}, ..., z_M^{\min})$, where $z_i^{\min}$ is the minimum value of the i-th objective. Next, the objective values of each scheme in S_g are transformed with respect to the ideal point as $F_i'(X) = F_i(X) - z_i^{\min}$. Subsequently, the extreme point ($z_i^{\max}$) on each (i-th) objective axis is determined, and the hyperplane is formed based on the M extreme points. Finally, the intercept a_i of each objective axis is obtained and the normalized objective value is obtained from Eq.(13).

$$F_i^n(X) = \frac{F_i'(X)}{a_i} \tag{13}$$

The normalized scheme in S_g in the hyperplane is associated with a reference point. First, the reference points are connected to the ideal points to form a reference vector. Second, the Euclidean distance between each individual and the reference vector is computed. Finally, each individual is associated with the nearest reference vector.

After associating the reference points with the scheme in S_g, the number of times the first $l-1$ layers of the schemes are associated with each reference point ρ_j is counted. Let $J_{\min} = \{j : \arg\min_j \rho_j\}$ be the set of reference points with the smallest ρ_j. Select the reference point $\bar{j} \in J_{\min}$.

If the selected $\rho_{\bar{j}} = 0$, no scheme is associated with $\bar{j}$ in the first $l-1$ layers. At this time, two choices are available. 1) A scheme in F_l that is associated with this reference point exists. At this time, the individual with the shortest distance

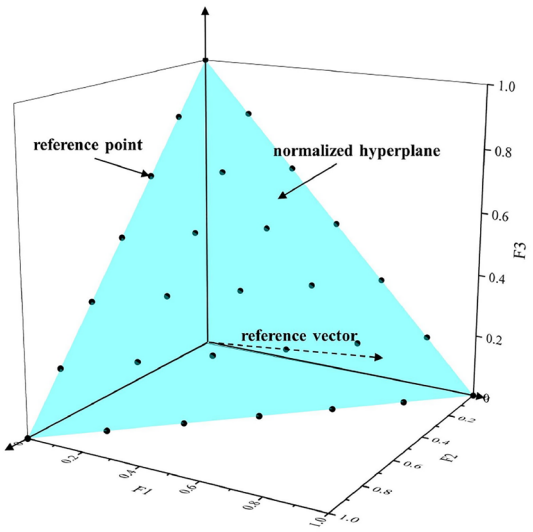

Fig. 4 (Color online) Reference points are shown on a normalized hyperplane for a three-objective problem with $p = 6$

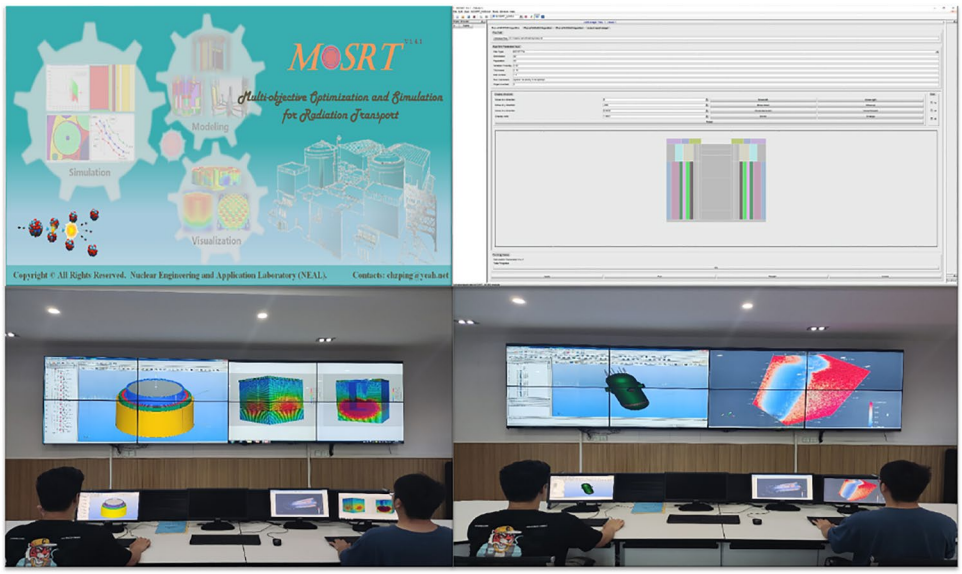

Fig. 5 (Color online) Radiation-shielding design optimization based on MOSRT software

from the reference vector Euclidean is selected to join the population, and at the same time, $\rho_{\bar{j}}$ is increased by 1. 2) If the reference point $\bar{j}$ does not have a scheme associated with it in F_l, then this reference point is skipped.

If $\rho_{\bar{j}} > 0$, then at least one scheme exists in the first l - 1 layers associated with $\bar{j}$. In this case, the scheme in $\bar{j}$ is chosen randomly to join the population, whereas $\rho_{\bar{j}}$ increases by one. The reference-point strategy ensures that the population is well distributed and can guide the evolution of the population to a uniform Pareto front.

4 Numerical evaluation for radiation-shielding-optimization problems

Two sets of numerical simulations are conducted, as follows:

(1) The GA and ABC algorithms are combined with Pareto-frontier-selection strategies based on the reference-point strategy or crowding-distance strategy, respectively, to test the optimization of a simple three-dimensional (3D) shielding problem, and the optimization performance of each strategy is compared.
(2) Constrained many-objective optimization of a complex shielding problem is conducted using the proposed optimization method and is compared with the initial shielding scheme.

In the following sections, we refer to the algorithms based on the reference-point-selection strategy as RP-NSGA and RP-MOABC, and those based on the crowding-distance strategy as CD-NSGA and CD-MOABC. The neutron database used in the simulation is ENDF/B-VIII.0 [36], and the photon database is MCPLIB84. The neutron flux-dose rate and photon flux-dose rate conversion factors used are NCRP-38 and ANSI/ANS 1977 [37], respectively. Particle-transport simulations are conducted using the Monte Carlo code MagicMC [38], and the overall optimization process, including evolutionary algorithms and the Monte Carlo code, is integrated into the self-developed software MOSRT (Fig. 5).

4.1 Many-objective optimization for a simple 3D shielding problem

The first problem focuses on the multiple objectives of a simple 3D shielding structure, as shown in Fig. 6a. The optimization objectives are to determine the total volume and weight of the R1-R10, U1-U5, and L1-L5 shielding layers as well as the radial lateral, axial upward, and axial downward dose rates of the shielding layers. The thickness of each shielding layer in the optimized model ranges from 0.3 cm to 13 cm. The reactor consists of a homogenized core with a height of 167.6 cm and radius of 78.8 cm. The source term is set as a fixed source with a probability distribution based on the Watt-fission spectrum. A comparative analysis of the optimization performance of each algorithm is performed using the average objective value and hypervolume [39] value.

In this problem, GA-based algorithms use binary encoding and ABC-based algorithms use real-number encoding. The population size of all algorithms is set to 210, and the number of reference points of the algorithms using the RP strategy is 210 (the number of divisions H=6). The number of MC transported particles is 1.0×10^7.

For the shielding-optimization process, the time complexity is mainly related to the number of evolutionary generations g and the population size N, where the total time

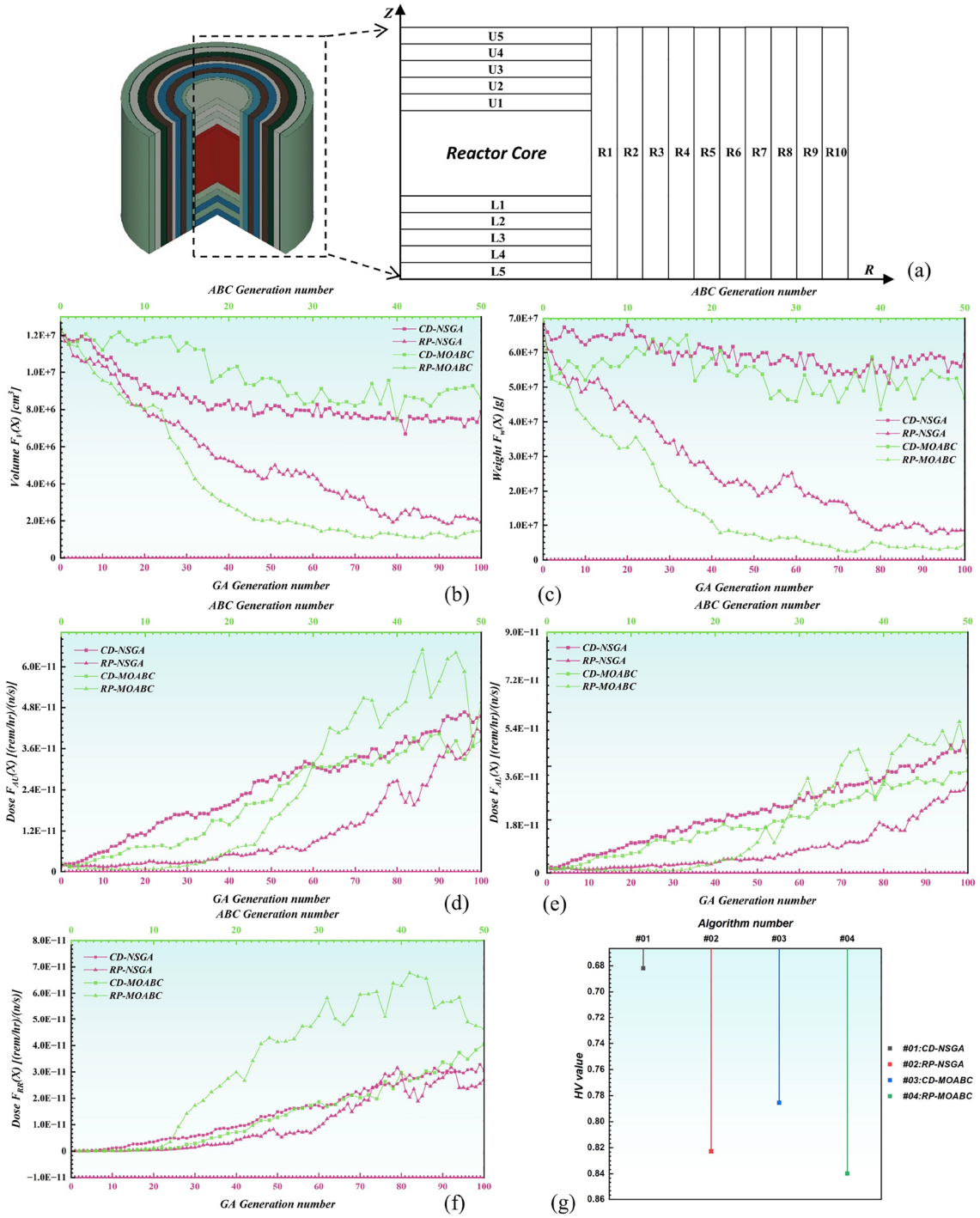

Fig. 6 (Color online) Many-objective optimization results for the simple 3D shielding problem. **a** Schematic of the simple 3D shielding structure. **b** The average values of the volumes for shielding schemes in the Pareto front. **c** The average values of the weights for shielding schemes in the Pareto front. **d** The average values of the axial upward dose rates for shielding schemes in the Pareto front. **e** The average values of the axial downward dose rates for shielding schemes in the Pareto front. **f** The average values of the radial dose rates for shielding schemes in the Pareto front. **g** Hypervolume indicator results

complexity of the GA is $O(gN)$ and that of the ABC algorithm is $O(2gN)$. To ensure that the tests are conducted under identical conditions, the number of evolutionary generations of the GA-based algorithms is set to 100, whereas that of ABC-based algorithm is 50.

As observed in the average objective values shown in Fig. 6b-f, the algorithms based on the reference-point strategy show excellent optimization results in terms of the weight and volume objectives. Compared with the conventional crowding-distance strategy, the average volume and weight values for the shielding schemes in the final generation of RP-NSGA are only 24.5% and 14.5% of those of CD-NSGA, and the average volume and weight values of RP-MOABC are only 17.3% and 9.77% of those of CD-MOABC. Regarding the dose rates in each region, the results in the final generation of each strategy are not significantly better or worse; the distribution of the results is relatively close, and the algorithm with relatively better performance is RP-NSGA. Overall, based on the average objective values, the algorithms using the reference-point strategy exhibit better convergence results.

To further evaluate the comprehensive performance of each algorithm scientifically, the hypervolume (HV) is chosen as the quantified factor to measure the convergence and distribution of the shielding schemes. The HV metric is a widely used performance evaluation method for engineering optimization problems and does not require a real Pareto front to judge the strengths and weaknesses of a set of population schemes. The HV metric is calculated as shown in Eq.(14):

$$HV = \delta\left(\bigcup_{i=1}^{S_i} v_i\right). \tag{14}$$

The combined performance of the algorithms can be determined by calculating the sum of the values of the hypervolume v_i in space for all the schemes in the population. The larger the combined value of the hypervolume, the better the performance. Figure 6g shows that the optimization performance from high to low follows the order of RP-MOABC, RP-NSGA, CD-MOABC, and CD-NSGA. The algorithms based on the reference-point strategy are comprehensively better than the conventional crowding-distance strategy for many-objective optimization problems.

4.2 Constrained many-objective optimization for a complex 3D shielding problem

The second problem focuses on conducting a constrained many-objective optimization for the complex shielding structures shown in Fig. 7a. For the constraint objectives, the thermal neutron-flux rate on the outermost shielding layer of the primary-shielding system must be less than 1.0×10^5 n/(cm^2 · s), the fast neutron-flux rate must be less than 1.0×10^3 n/(cm^2 · s), and the gamma-ray energy-flux rate must be less than 6.0×10^6 MeV/(cm^2 · s). The optimization objectives include the total volume and weight of shielding layers R1–R8 and U1–U3, as well as the dose rates in the radial and axial upward directions of the shielding layers. The variable parameters are the shielding-layer thickness, shielding-layer materials, and partial material compositions (boron polyethylene, lead boron polyethylene, tungsten alloy). The thickness of each shielding layer in the optimized model ranges from 15 cm to 80 cm. The reactor consists of a homogenized core with a height of 167.6 cm and radius of 78.8 cm. The source term is set as a fixed source with a probability distribution based on the Watt-fission spectrum.

In this problem, GA- and ABC-based algorithms use real-number encoding. The population size of all the algorithms is set to 100, and the number of reference points of the algorithms using the RP strategy is 84. (The number of divisions H=6.) The number of MC transported particles is 2.0×10^8. For computational efficiency, eight AMD EPYC 7H12 CPUs (Dual 128 core, 2.6 GHz) are used for massive parallel computation.

A heat map of the optimization ratio is plotted for the last generation of optimized shielding schemes compared to the initial shielding scheme, where the optimization ratio is defined in Eq.(15):

$$\begin{aligned} &\text{improvements} = \frac{\left(F_{\text{initial},j} - F_{i,j}\right)}{F_{\text{initial},j}} \times 100\% \\ &i = 1, ..., N j = 1, ..., M \end{aligned}. \tag{15}$$

In Eq. (15), i represents the individual index, N represents the population size, j represents the dimension of the objective values, M represents the total number of objective values, and F represents the corresponding objective values. A higher value of the optimization ratio indicates a better optimization of the corresponding objective. Figure 7b-e shows that the optimization effect of each method is obvious in the three objective dimensions of volume, weight, and radial dose rate. However, for the top-side dose rate, some of the schemes show a degree of degradation, but they still achieve a better scheme set compared to the initial shielding scheme. The optimization performances of RP-NSGA and RP-MOABC in each objective dimension are better than those of CD-NSGA and CD-MOABC, which proves that the algorithms proposed in this study are feasible for many-objective optimization problems.

In practical engineering shielding-design problems, the final design scheme can be selected from a Pareto set of optimization schemes based on specific requirements. In this study, the miniaturization schemes obtained by the RP-NSGA algorithm (Shield #1) and RP-MOABC algorithm (Shield #2) are selected for demonstration. The shielding structure is shown in Fig. 8b-c, the dose field distribution is shown in Fig. 8d-e, and the specific parameters and optimization effects are listed in Tables 1, 2, 3 and 4. The dose rates are computed with the MagicMC Monte Carlo code using the global variance-reduction method [40–43] with a statistical error of less than 5%.

Table 1 Component ratios of various materials for each optimized shielding scheme

Shielding Scheme No.	Borated Polyethylene		Lead-Borated Polyethylene			Tungsten Alloy		
	B_4C (%)	PE (%)	Pb (%)	B_4C (%)	PE (%)	W (%)	Ni (%)	Fe (%)
Initial shield	80.30	19.70	53.17	2.34	44.49	98.66	0.94	0.40
Shield #1	76.85	23.15	80.17	0.99	18.83	90.53	6.63	2.84
Shield #2	30.34	69.66	90.00	0.50	9.50	90.62	6.57	2.81

Table 2 Objective values and optimization ratios of the optimized shielding schemes

Shielding Scheme No.	Volume		Weight		Radial dose rate		Axial upper dose rate	
	Numeric (cm^3)	OR (%)	Numeric (g)	OR (%)	Numeric (rem/hr)	OR (%)	Numeric (rem/hr)	OR (%)
Initial shield	1.01×10^8	–	9.11×10^8	–	9.90×10^0	–	9.95×10^{-1}	–
Shield #1	8.17×10^7	18.95	4.44×10^8	51.19	9.36×10^0	5.44	7.75×10^{-1}	22.09
Shield #2	8.15×10^7	19.12	6.88×10^8	24.50	9.77×10^0	1.32	5.31×10^{-1}	46.62

Table 3 Numerical values of constrained objectives for the optimized shielding schemes

Shielding Scheme No.	Radial outermost shield			Axial topmost shield		
	Thermal neutron ($n/(cm^2 \cdot s)$)	Fast neutron ($n/(cm^2 \cdot s)$)	Photon ($MeV/(cm^2 \cdot s)$)	Thermal neutron ($n/(cm^2 \cdot s)$)	Fast neutron ($n/(cm^2 \cdot s)$)	Photon ($MeV/(cm^2 \cdot s)$)
Initial shield	1.06×10^2	6.15×10^2	3.56×10^5	1.94×10^2	7.39×10^1	5.35×10^5
Shield #1	6.01×10^{-2}	3.57×10^0	5.28×10^5	2.53×10^0	2.53×10^0	2.88×10^5
Shield #2	2.34×10^1	3.02×10^2	3.95×10^5	5.96×10^0	1.81×10^2	1.01×10^5

Table 4 Design parameters of the optimization schemes

Shielding layer No.	Initial shield		Shield #1		Shield #2	
	Thickness (cm)	Material type	Thickness (cm)	Material type	Thickness (cm)	Material type
R1	28.7	B-Steel	28.2	Pb-B-PE	40.0	Pb-B-PE
R2	25.8	Pb-B-PE	33.3	Pb-B-PE	40.0	B_4C
R3	35.4	W-Ni-Fe	34.7	W-Ni-Fe	29.8	H_2O
R4	32.2	Pb-B-PE	31.0	B_4C	15.0	W-Ni-Fe
R5	36.9	W-Ni-Fe	33.2	B-PE	40.0	W-Ni-Fe
R6	21.8	W-Ni-Fe	22.0	Pb-B-PE	15.0	Pb-B-PE
R7	50.0	Pb-B-PE	20.0	W-Ni-Fe	20.0	B-Steel
R8	66.8	H_2O	20.3	H_2O	20.0	B-PE
U1	34.1	W-Ni-Fe	64.3	W-Ni-Fe	74.4	W-Ni-Fe
U2	58.0	H_2O	78.5	H_2O	80.0	W-Ni-Fe
U3	46.4	Air	20.0	Air	20.0	Air

5 Conclusion

With the development of new nuclear-reactor types, this study introduces two many-objective evolutionary algorithms based on a reference-point-selection strategy and applies them to many-objective radiation-shielding-optimization problems. The basic principles of the proposed evolutionary algorithms for shielding optimization are described

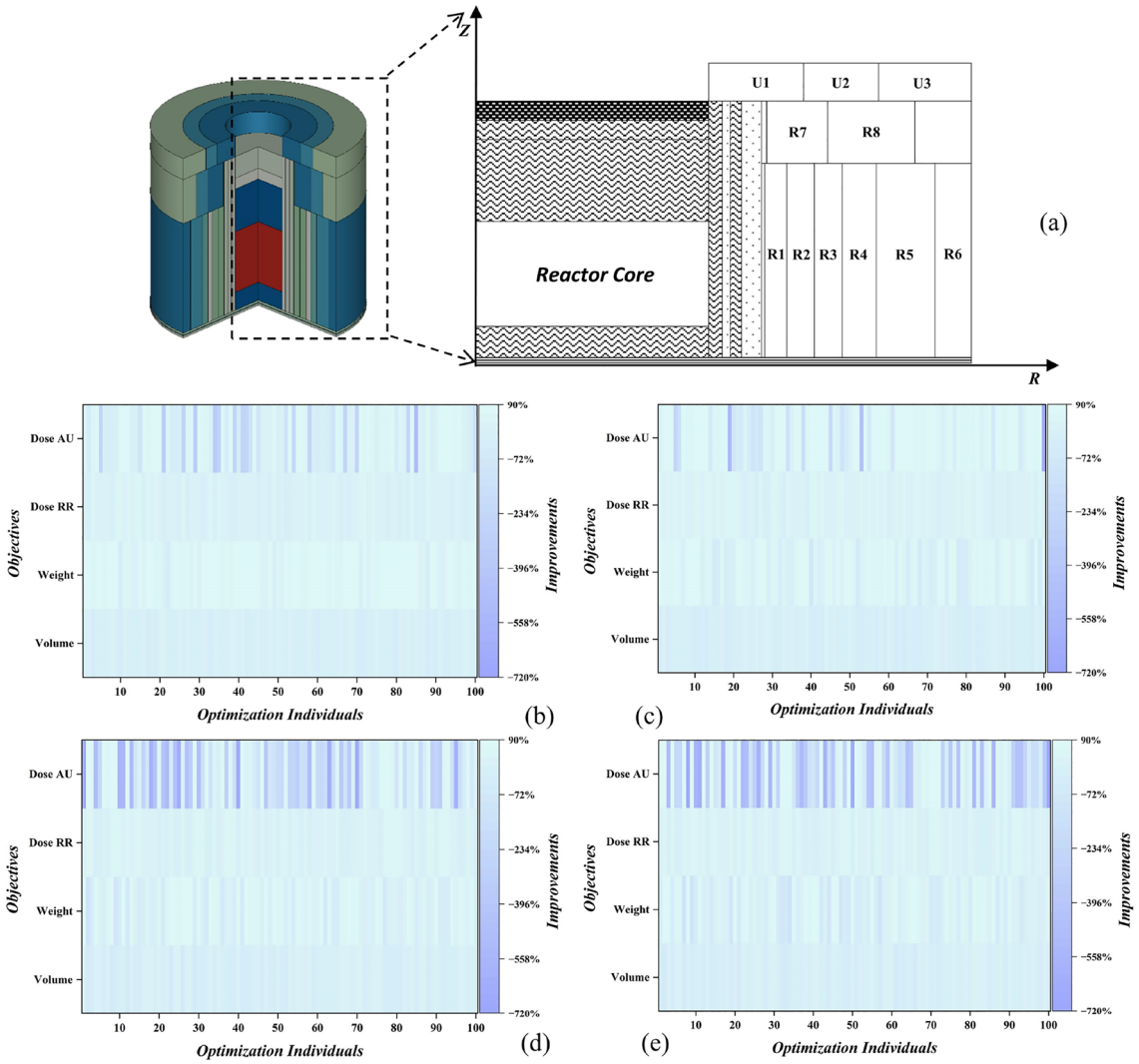

Fig. 7 (Color online) Constrained many-objective optimization results for complex shielding structure. **a** Schematic of the complex shielding structure. **b** Improvements of the optimized objectives with RP-NSGA. **c** Improvements of the optimized objectives with RP-MOABC. **d** Improvements of the optimized objectives with CD-NSGA. **e** Improvements of the optimized objectives with CD-MOABC

in detail. The algorithms efficiently and accurately deliver an optimal set of shielding schemes that are more compact and lightweight and have lower dose rates. This study conducts a performance assessment based on a simple 3D shielding problem, with the results indicating superiority over evolutionary algorithms that rely on crowding-distance strategies. However, for the optimization of a complex shielding problem with multiple constraints for practical applications, the algorithms proposed in this study are able to obtain optimized design schemes with superior objective values compared to the initial scheme. Furthermore, by incorporating the composition of the shielding materials into the optimization process, the algorithms enhance the diversity and creativity of the shielding design. In summary, optimization algorithms can effectively identify excellent shielding schemes in the early stages of radiation-shielding design for nuclear reactors. This study provides significant guidance for radiation-shielding design and provides supplementary data during the conceptual design phase of novel nuclear facilities with limited engineering experience.

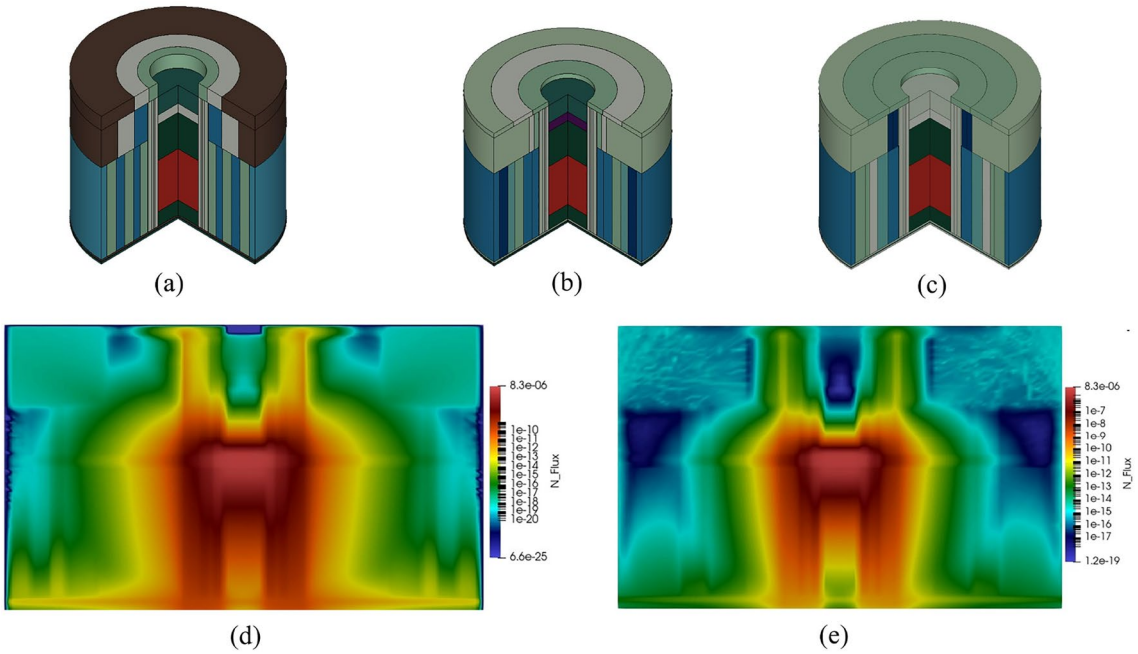

Fig. 8 (Color online) Schematic of typical shielding schemes after optimization. **a** Initial shielding structure. **b** Miniaturization scheme of RP-NSGA. **c** Miniaturization scheme of RP-MOABC. **d** Dose field distribution of the RP-NSGA miniaturization scheme. **e** Dose field distribution of the RP-MOABC miniaturization scheme

Author contributions All authors contributed to the study conception and design. Material preparation, data collection, and analysis were performed by Cheng-Wei Liu, Ai-Kou Sun, Hong-Yu Qu, and Zhen-Ping Chen. The first draft of the manuscript was written by Cheng-Wei Liu, and all authors commented on previous versions of the manuscript. All authors read and approved the final manuscript.

Data availability The data that support the findings of this study are openly available in Science Data Bank at https://cstr.cn/31253.11.sciencedb.j00186.00575 and https://doi.org/10.57760/sciencedb.j00186.00575.

Declarations

Conflict of interest The authors declare that they have no conflict of interest.

References

1. Y. Chen, B. Yan, The technology of shielding design for nuclear reactor: a review. Prog. Nucl. Energ. **161**, 104741 (2023). https://doi.org/10.1016/j.pnucene.2023.104741
2. N.M. Schaeffer, *Reactor Shielding for Nuclear Engineers* (US Atomic Energy Commission Office of Information Services, 1983). https://doi.org/10.2172/4479460
3. S.F. Demuth, SP100 space reactor design. Prog. Nucl. Energ. **42**(3), 323–59 (2003). https://doi.org/10.1016/S0149-1970(03)90003-5
4. Y. Wang, Y. Tao, Y. Tao et al., Shielding design of a megawatt-scale heat pipe reactor core. Nucl. Tech. (in Chinese) **46**(02), 020606 (2023). https://doi.org/10.11889/j.0253-3219.2023.hjs.46.020606.
5. M.A. Sazali, N. Rashid, K. Hamzah, A preliminary study to metaheuristic approach in multilayer radiation shielding optimization. Mater. Sci. Eng. **298**(1), 012042 (2018). https://doi.org/10.1088/1757-899X/298/1/012042/meta
6. B.S. Skim, J.H. Moon, Use of a genetic algorithm in the search for a near-optimal shielding design. Ann. Nucl. Energy **37**(2), 120–129 (2010). https://doi.org/10.1016/j.anucene.2009.11.014
7. S. Zheng, Q. Pan, H. Lv et al., Semi-empirical and semi-quantitative lightweight shielding design method. Nucl. Sci. Tech. **34**(3), 43 (2023). https://doi.org/10.1007/s41365-023-01187-2
8. Z. Chen, Z. Zhang, J. Xie et al., Metaheuristic optimization method for compact reactor radiation shielding design based on genetic algorithm. Ann. Nucl. Energy **134**, 318–329 (2019). https://doi.org/10.1016/j.anucene.2019.06.031
9. J. Lei, C. Yang, H. Zhang et al., Radiation shielding optimization design research based on bare-bones particle swarm optimization algorithm. Nucl. Eng. Technol. **55**(6), 2215–2221 (2023). https://doi.org/10.1016/j.net.2023.02.018
10. Y. Song, J. Mao, Z. Zhang et al., A novel multi-objective shielding optimization method: DNN-PCA-NSGA-II. Ann. Nucl. Energy **161**, 108461 (2021). https://doi.org/10.1016/j.anucene.2021.108461
11. Z. Chen, Z. Zhang, J. Xie et al., Multi-objective optimization strategies for radiation shielding design with genetic algorithm. Comput. Phys. Commun. **260**, 107267 (2021). https://doi.org/10.1016/j.cpc.2020.107267
12. C. He, X. Qiu, Z. Sun et al., Radiation shielding optimization of space reactor based on intelligent decision support system. Nucl. Tech. (in Chinese) **45**(05), 050601 (2022). https://doi.org/10.11889/j.0253-3219.2022.hjs.45.050601.
13. K. Li, R. Wang, T. Zhang et al., Evolutionary many-objective optimization: A comparative study of the state-of-the-art. IEEE Access **6**, 26194–26214 (2018). https://doi.org/10.1109/ACCESS.2018.2832181

14. H. Chen, Y. Tian, W. Pedrycz et al., Hyperplane assisted evolutionary algorithm for many-objective optimization problems. IEEE T. Cybernetics. **50**(7), 3367–3380 (2020). https://doi.org/10.1109/TCYB.2019.2899225
15. K. Li, K. Deb, Q. Zhang et al., An evolutionary many-objective optimization algorithm based on dominance and decomposition. IEEE T. Evolut. Comput. **19**(5), 694–716 (2014). https://doi.org/10.1109/TEVC.2014.2373386
16. H. Ishibuchi, N. Tsukamoto, Y. Nojima, Evolutionary many-objective optimization: A short review. IEEE C. Evol. Computat. pp. 2419-2426 (2008). https://doi.org/10.1109/CEC.2008.4631121
17. G. Hu, H. Hu, Q. Yang et al., Study on the design and experimental verification of multilayer radiation shield against mixed neutrons and γ-rays. Nucl. Eng. Technol. **52**(1), 178–184 (2020). https://doi.org/10.1016/j.net.2019.07.016
18. H.O. Tekin, T. Manici, Simulations of mass attenuation coefficients for shielding materials using the MCNP-X code. Nucl. Sci. Tech. **28**, 95 (2017). https://doi.org/10.1007/s41365-017-0253-4
19. J. Zhou, Q. Zeng, Y. Xiong et al., Research on the shielding performance and optimization of new type foam metal matrix composite shielding materials. Nucl. Instrum. Meth. B. **516**, 31–37 (2022). https://doi.org/10.1016/j.nimb.2022.02.005
20. Y. Tian, X. Zhang, R. Cheng et al., Guiding evolutionary multiobjective optimization with generic front modeling. IEEE T. Cybernetics. **50**, 1106–1119 (2020). https://doi.org/10.1109/TCYB.2018.2883914
21. F. Chen, G. Li, M. Yang, Y. Han, R. Liang, Optimization research on neutron shielding material component based on genetic algorithm. Radiat. Prot. **40**(1), 38–44 (2020). (in Chinese)
22. Y. Li, T. Yu, Z. Chen et al., Development and verification of radiation shielding optimization design platform for marine reactor. Nuclear Power Eng. **43**(1), 221–228 (2022). https://doi.org/10.13832/j.jnpe.2022.01.0208 (in Chinese)
23. L. Kuang, T. Yu, Z. Chen et al., CAD-based inversion visualization of monte Carlo Computational model based on SALOME. High Power Laser Particle Beams. **35**(03), 168–174 (2023). https://doi.org/10.11884/HPLPB202335.220276 (in Chinese)
24. Y. Hu, Y. Qiu, U. Fischer, Development and benchmarking of the Weight Window Mesh function for OpenMC. Fusion Eng. Des. **170**, 112551 (2021). https://doi.org/10.1016/j.fusengdes.2021.112551
25. I. Das, J.E. Dennis, Normal-boundary intersection: a new method for generating the Pareto surface in nonlinear multicriteria optimization problems. Siam. J. Optimiz. **134**, 631–657 (1998). https://doi.org/10.1137/S1052623496307510
26. K. Deb, A. Pratap, S. Agarwal et al., A fast and elitist multi objective genetic algorithm: NSGA-II. IEEE T. Evolue. Comput. **6**(2), 182–197 (2002). https://doi.org/10.1109/4235.996017
27. K.S. Tang, K.F. Man, S. Kwong et al., Genetic algorithms and their applications. IEEE Signal. Proc. Mag. **13**(6), 22–37 (1996). https://doi.org/10.1109/79.543973
28. H. Zhang, Z. Chen, C. Liu et al., Study on many-objective optimization method for reactor 3D shielding structure based on genetic algorithm. Nucl. Tech. (in Chinese) **45**(11), 110603 (2022). https://doi.org/10.11889/j.0253-3219.2022.hjs.45.110603
29. Y. Xiang, Y. Zhou, H. Liu, An elitism based multi-objective artificial bee colony algorithm. Eur. J. Oper. Re. **245**(1), 168–193 (2015). https://doi.org/10.1016/j.ejor.2015.03.005
30. R. Akbari, R. Hedayatzadeh, K. Ziarati et al., A multi-objective artificial bee colony algorithm. Swarm Evol. Comput. **2**, 39–52 (2012). https://doi.org/10.1016/j.swevo.2011.08.001
31. F. Neri, V. Tirronen, Recent advances in differential evolution: a survey and experimental analysis. Artif. Intell. Rev. **33**, 61–106 (2010). https://doi.org/10.1007/s10462-009-9137-2
32. E. Tanyildizi, G. Demir, Golden sine algorithm: A novel math-inspired algorithm. Adv. Electr. Comput. En. **17**, 71–78 (2017). https://doi.org/10.4316/AECE.2017.02010
33. Q. He, L. Wang, A hybrid particle swarm optimization with a feasibility-based rule for constrained optimization. Appl. Math. Comput. **186**(2), 1407–1422 (2007). https://doi.org/10.1016/j.amc.2006.07.134
34. H. Jain, K. Deb, An evolutionary many-objective optimization algorithm using reference-point based nondominated sorting approach, part II: Handling constraints and extending to an adaptive approach. Ieee. T. Evolue. Comput. **18**(4), 602–622 (2013). https://doi.org/10.1109/TEVC.2013.2281534
35. K. Deb, H. Jain, An evolutionary many-objective optimization algorithm using reference-point-based nondominated sorting approach, part I: solving problems with box constraints. IEEE T. Evolue. Comput. **18**(4), 577–601 (2013). https://doi.org/10.1109/TEVC.2013.2281535
36. D.A. Browm, M.B. Chadwick, R. Capote et al., ENDF/B-VIII. 0: the 8th major release of the nuclear reaction data library with CIELO-project cross sections, new standards and thermal scattering data. Nucl. Data Sheets **148**, 1–142 (2018). https://doi.org/10.1016/j.nds.2018.02.001
37. Y. Harima, An historical review and current status of buildup factor calculations and applications. Radiat. Phys. Chem. **41**, 631–672 (1993). https://doi.org/10.1016/0969-806X(93)90317-N
38. A. Sun, Z. Chen, T. Yu et al., Development and verification of a monte carlo calculation program magic for dose of boron neutron capture therapy. Modern Appl. Phys. **14**(04), 41–48 (2023). https://doi.org/10.12061/j.issn.2095-6223.2023.040202 (in Chinese)
39. Z. Yang, H. Wang, K. Yang, SMS-EMOA: Multiobjective selection based on dominated hypervolume. IEEE World Cong. Comput. Intel. pp. 282–288 (2016). https://doi.org/10.1109/FSKD.2016.7603187
40. Q. Pan, N. An, T. Zhang et al., Single-step Monte Carlo criticality algorithm. Comput. Phys. Commun. **279**, 108439 (2022). https://doi.org/10.1016/j.cpc.2022.108439
41. Q. Pan, H. Lv, S. Tang et al., Pointing probability driven semi-analytic Monte Carlo method (PDMC)-Part I: global variance reduction for large-scale radiation transport analysis. Comput. Phys. Commun. **291**, 108850 (2023). https://doi.org/10.1016/j.cpc.2023.108850
42. Q. Pan, T. Zhang, X. Liu et al., SP3-coupled global variance reduction method based on RMC code. Nucl. Sci. Tech. **32**, 122 (2021). https://doi.org/10.1007/s41365-021-00973-0
43. L. Li, S. Jiang, Z. Chen et al., Mesh-based activation analysis for structural materials in nuclear reactor. Nucl. Tech. (in Chinese) **45**(08), 080601 (2022). https://doi.org/10.11889/j.0253-3219.2022.hjs.45.080601.